Modelisation of transition and noble metal vicinal surfaces: energetics, vibrations and stability

Cyrille Barreteau, Faical Raouafi, Marie-Catherine Desjonquères, Daniel Spanjaard

Modelisation of transition and noble metal vicinal surfaces: energetics, vibrations and stability

C. Barreteau*, F. Raouafi*, M.C. Desjonquères* and D. Spanjaard†

*DSM/DRECAM/SPCSI, CEA Saclay
F-91 191 Gif sur Yvette, France
†Laboratoire de Physique des Solides, Université Paris Sud, F-91 405 Orsay, France

Abstract. The energetics of transition and noble metal (Rh, Pd, Cu) vicinal surfaces, i.e., surface energy, step energy, kink energy and electronic interactions between steps, is studied at 0K from electronic structure calculations in the tight-binding approximation using a *s, p* and *d* valence orbital basis set. Then, the surface phonon spectra of copper are investigated in the harmonic approximation with the help of a semi-empirical inter-atomic potential. This allows to derive the contribution of phonons at finite temperatures to the step free energy and to the interactions between steps. The last part is devoted to the stability of vicinal surfaces relative to faceting with special attention to the domain of orientations (100)-(111). Semi-empirical potentials are shown to be not realistic enough to give a reliable answer to this problem. The results derived from electronic structure calculations predict a variety of behaviors and, in particular, a possible faceting into two other vicinal orientations. Finally, temperature effects are discussed. Comparisons are made with other theoretical works and available experiments.

PACS numbers: 68.35.Ja, 68.35.Md, 65.40.Gr, 68.35.Rh, 71.15.Nc

1. Introduction

Studies of vicinal surfaces of metals have given rise to numerous experimental and theoretical works. Indeed the role of steps and kinks is fundamental for understanding the morphology of crystal surfaces and, in particular, its evolution with time and temperature as well as the equilibrium surface structure. In addition, vicinal surfaces may provide appropriate substrates for growing nanostructures, for instance nanowires, with magnetic and transport properties of high technological interest.

In the last twenty years the direct investigation of the local surface structure has become possible by the use of scanning probe microscopies such as the Scanning Tunneling Microscope (STM). Information on the energetics of surface defects can henceforth be derived from a statistical study of STM images and their evolution with temperature. For instance, the study of the equilibrium shape of large adislands grown in homoepitaxy on monocrystalline surfaces has been used to determine the anisotropy of step energies and, more recently, the absolute values of step and kink energies [1]. Furthermore, the interaction between steps can be deduced from the study of terrace width distributions [2]. Kink energies can also be obtained from the observation of the spatial equilibrium fluctuations of step edges [3, 4]. In addition experimental investigations of localized vibrational modes at vicinal surfaces have been carried out in the last decade by Inelastic Helium Atom Scattering (IHAS)[5] or Electron Energy Loss Spectroscopy (EELS)[6].

All these experimental results have motivated a lot of theoretical works. The study of the energetics of vicinal surfaces at 0K starts from the determination of the surface energies as a function of the surface orientation. It has been investigated either by using semi-empirical potentials including an N-body contribution such as Effective Medium Theory (EMT)[7, 8], Embedded Atom Method (EAM)[9], Second Moment Potential (SMA)[10, 11, 12], or starting from the determination of the electronic structure using

the Density Functional Theory (DFT) or the Tight Binding approximation (TB). However, due to the very low symmetry of these systems, first principle calculations are scarce and limited to a very small number of geometries and metals: Al [13, 14], Cu [15, 16], Pt [17]. On the contrary, in the case of transition metals, TB methods are able to describe correctly the quantum mechanical effects without a lot of computational efforts. Using this method we have been able [18] to perform a systematic study of various vicinal surfaces of Rh, Pd and Cu as a function of the misorientation angle from which we have deduced step and kink energies as well as step-step interactions. The results of this work are reviewed in Sect.3, after a brief presentation of the geometry of vicinal surfaces (Sect.2).

Similarly ab-initio methods have also been used to obtain localized vibration modes at vicinal surfaces but only the modes at high symmetry points of the Brillouin zone have been investigated [19, 20]. Central pair potentials in the harmonic approximation yield a reasonable description of vibration modes but not at a quantitative level. A good accuracy can be achieved with N-body semi-empirical potentials such as EAM [21, 22]. More recently we have set up a new potential for Cu [23] with which we have been able to reproduce accurately the phonon dispersion curves measured by IHAS [5] and EELS [6] on flat as well as on vicinal surfaces. In Sect.4 this potential is presented and the results concerning phonon dispersion curves and the vibrational contribution to the step free energy are summarized.

Finally, it is not obvious that all vicinal surfaces should be in thermodynamic equilibrium. Actually vicinal surfaces may decrease their surface free energy by rearranging the atoms in order to exhibit a hill and valley (or a factory roof) structure. This phenomenon, called faceting, is indeed observed in experiments and its occurrence can be predicted from the knowledge of the spatial anisotropy of the surface energy [24]. Using the results of Sects.3 and 4. we have been able to reexamine [25, 26] in a realistic way this old problem. In Sect.5 we report our main results and discuss the implications of doing electronic structure calculations rather than using empirical potentials.

2. The geometry of vicinal surfaces

A vicinal surface is obtained by cutting a crystal along a plane making an angle θ with respect to a low index plane normal to the direction $\mathbf{n_0}$ (Fig.1). For selected values of θ, such a surface can be viewed as a periodic succession of terraces normal to $\mathbf{n_0}$, with equal widths, separated by steps of monoatomic height. The width of the terraces is determined by the number p of atomic rows (including the inner edge) parallel to the step edges. A vicinal surface corresponds to an atomic plane with high Miller indices. It can also be denoted using the Lang et al. [27] notation $p(hkl) \times (h'k'l')$, (hkl) and $(h'k'l')$ being respectively the Miller indices of planes parallel to the terraces and to the ledges. Note also that when projecting the unit cell of the vicinal surface on the terrace plane, a geometrical factor f occurs when the ledges and the terraces are not orthogonal.

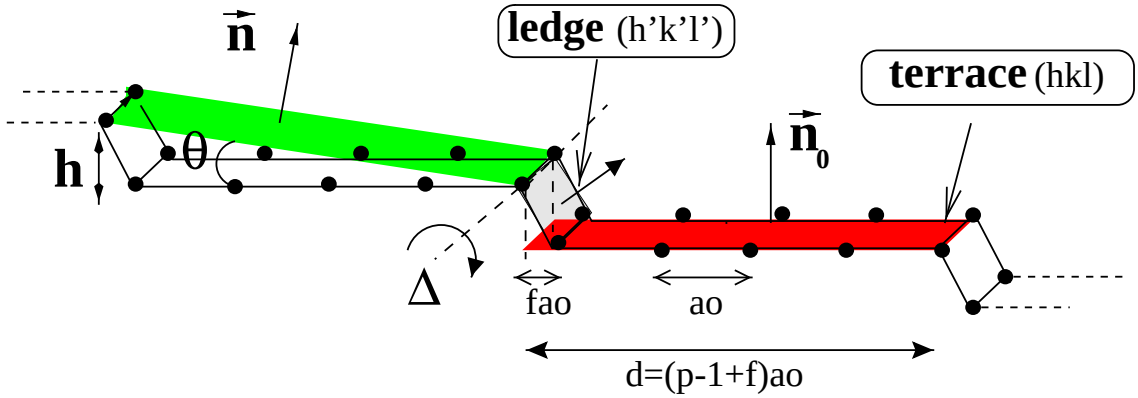

Figure 1. Step geometry of a $p(hkl) \times (h'k'l')$ vicinal surface

Lang et al. notations	Miller indices	f	Edge geometry	2D unit cell
$p(111) \times (100)$ step A	$(p+1, p-1, p-1)$	2/3	nn	p odd: PR p even: CR
$p(111) \times (\bar{1}11)$ step B	$(p-2, p, p)$	1/3	nn	p odd: CR p even:PR
$p(100) \times (111)$	$(1, 1, 2p-1)$	1/2	nn	CR
$p(100) \times (010)$	$(0, 1, p-1)$	0	nnn	p odd: CR p even: PR

Table 1. Geometrical features of the four types of vicinal surfaces. The geometry of the step edges is indicated by the distance between two consecutive atoms: nearest neighbors (nn), next nearest neighbors (nnn). The nature of the 2D unit cell is rectangular, either primitive (PR) or centered (CR). Finally the usual notations, step A and step B, for the vicinals of (111) are indicated

In the following we consider FCC crystals and four step geometries with (111) and (100) terraces. The geometrical features of the four types of vicinal surfaces, denoted using Lang et al. notations and Miller indices, are given in Table 1. One can note that for a given step geometry there often exists two types of unit cell (primitive rectangular and centered rectangular) depending on the width of the terrace (p even or odd). In the first three considered geometries, the atoms along the step edges are first nearest neighbors while for the $p(100) \times (010)$ surface the atoms are second nearest neighbors and, consequently, the corresponding step edge has a zigzag shape that can be seen as a succession of kinks.

3. Electronic structure and energetics of vicinal surfaces in a tight-binding model.

3.1. The spd tight-binding model.

The study of the electronic structure of vicinal surfaces has been carried out using a slab model. The orientation of the normal to the vicinal surface is first chosen. A succession of N_{slab} atomic layers is built, N_{slab} being large enough so that the interaction between the two free surfaces of the slab is negligible. The wider the terraces (i.e., the area of the vicinal surface unit cell), the smaller the inter-layer spacing and the larger the number of layers N_{slab}. The system has thus a two-dimensional periodicity with N_{slab} atoms per unit cell. Ab-initio calculations are in principle feasible. However they are, at least up to now, limited to small terrace widths since they need a large amount of computer time. On the contrary the TB scheme is very attractive since it is much less costly in computer time and still describes systems within the framework of quantum mechanics. Up to the last decade, the TB basis set was limited to the valence d $(xy, yz, zx, x^2-y^2, 3z^2-r^2)$ orbitals and this scheme was quite successful to explain the general trends in the variation of a large number of physical properties along the transition series. However for FCC elements at the end of these series, the values of energetic quantities are then underestimated, and even cancel for a full d band, due to the neglect of the contribution of the outer s and $p(x, y, z)$ orbitals. Recently, it was found that it is possible to determine a transferable parametrized TB hamiltonian in a *spd* basis set giving not only a quite good description of the band structure up to a few eV above the d band, but also total energies with a good accuracy. This was initially proposed by Mehl and Papaconstantopoulos who assumed a non orthogonal basis set [28]. Then it was shown [29] that for elements with a not completely filled d band, it was possible to reduce considerably the number of parameters by assuming an orthogonal basis set.

These models have been described in details in Refs [28, 29] thus their main features are only briefly recalled in the following. The interatomic matrix elements of the hamiltonian $H_{ij}^{\lambda\mu}$ (i,j: atomic sites, λ, μ: atomic orbitals) in the two-center approximation are determined from the ten Slater-Koster (SK) [30] hopping integrals $ss\sigma, sp\sigma, sd\sigma, pp\sigma, pp\pi, pd\sigma, pd\pi, dd\sigma, dd\pi, dd\delta$. The laws of variation with distance of the SK hopping integrals are a simple exponential decay in Ref.[29] and are slightly more involved with a larger number of parameters in Ref.[28]. In the non-orthogonal scheme the overlap integrals $S_{ij}^{\lambda\mu}$ introduce also ten SK-like overlap parameters and their variations with distance follow the same kind of laws as the interatomic matrix elements of H. Following Ref.[28], in both schemes the intra-atomic matrix elements $H_{ii}^{\lambda\lambda}$, i.e., the atomic levels $\varepsilon_s, \varepsilon_p, \varepsilon_d$, are defined in such a way that the total energy is obtained by summing up the occupied energy levels. This means that all the other terms contained in the energy functional of the DFT have been taken into account by a rigid shift of the bulk band structure. As a consequence the atomic levels should depend on the atomic

environment and are written in the form:

$$\varepsilon^0_{i\lambda} = a_\lambda + b_\lambda \rho_i^{2/3} + c_\lambda \rho_i^{4/3} + d_\lambda \rho_i^2 \tag{1}$$

with

$$\rho_i = \sum_{j \neq i} exp(-p_\rho(R_{ij}/R_0 - 1)) \tag{2}$$

where R_{ij} is the distance between atoms i and j and R_0 is a reference distance, usually the bulk equilibrium interatomic spacing.

The parameters of the model are determined by a non-linear least mean square fit on ab-initio band structure and total energy for a few crystallographic bulk structures (usually FCC and BCC) at several interatomic distances. Their values for Palladium and Rhodium have been given in Ref.[29, 31] and for Copper in Ref.[28, 32].

It should be noted that these parameters are obtained from systems in which all atoms are neutral since they are geometrically equivalent. When this is not the case we have added a shift δV_i to the on-site terms in order to ensure local charge neutrality which should be almost strictly obeyed in metals. Note that in the non-orthogonal case this induces also a modification $\delta V_{ij}^{\lambda\mu}$ of the interatomic elements of H [18]. These potentials arise from electron-electron interactions, thus one should subtract the corresponding double counting terms from the sum of occupied levels in the expression of the total energy which is then written in both schemes as:

$$E_{tot} = \sum_{nocc} \epsilon_n - N_{val} \sum_i \delta V_i \tag{3}$$

where N_{val} is the total number of valence *spd* electrons per atom of the metal.

3.2. The electronic structure

In order to apply the two-dimensional Bloch theorem, a basis set of 2D Bloch waves localized in each layer l is defined as follows:

$$B_{l\lambda}(\mathbf{r}, \mathbf{k}_{//}) = N_S^{-1/2} \sum_{i \in l} exp(i\mathbf{k}_{//}.\mathbf{R}_{i//}) |i\lambda > \tag{4}$$

where N_S is the number of atoms in each layer and $\mathbf{R}_{i//}$ the translation vectors of the two-dimensional (2D) lattice. Using this basis set the solution of the Schrödinger equation can be written:

$$\Psi_{\mathbf{k}_{//},n}(\mathbf{r}) = \sum_{l\lambda} c^n_{l\lambda}(\mathbf{k}_{//}) B_{l\lambda}(\mathbf{r}, \mathbf{k}_{//}) \tag{5}$$

and the hamiltonian and overlap matrices are reduced to $(9N_{slab} \times 9N_{slab})$ matrices $H^{\lambda\mu}_{ll'}$ $(\mathbf{k}_{//})$ and $S^{\lambda\mu}_{ll'}(\mathbf{k}_{//})$. Then the equation:

$$\sum_{l'\mu} [H^{\lambda\mu}_{ll'}(\mathbf{k}_{//}) - \epsilon_n(\mathbf{k}_{//}) S^{\lambda\mu}_{ll'}(\mathbf{k}_{//})] c^n_{l'\mu}(\mathbf{k}_{//}) = 0 \tag{6}$$

is solved. Note that when the basis is orthonormal this equation reduces to a classical eigenvalue(vector) problem. In order to determine the projected band structure $\epsilon_n(\mathbf{k}_{//})$, $\mathbf{k}_{//}$ is varied along symmetry lines of the surface Brillouin zone (SBZ). Other interesting quantities can be calculated such as the local density of states (LDOS) at layer l (per surface atom).

$$n_l(E) = \sum_{\substack{\lambda,n \\ l',\mu}} \frac{A}{(2\pi)^2} \int_{SBZ} c_{l\lambda}^{n*}(\mathbf{k}_{//}) S_{ll'}^{\lambda\mu}(\mathbf{k}_{//}) c_{l'\mu}^{n}(\mathbf{k}_{//}) \delta(E-\epsilon_n) d^2\mathbf{k}_{//} \tag{7}$$

where A is the area of the surface unit cell, or the spectral local DOS (per surface atom)

$$n_l(E, \mathbf{k}_{//}) = \sum_{\substack{\lambda,n \\ l',\mu}} c_{l\lambda}^{n*}(\mathbf{k}_{//}) S_{ll'}^{\lambda\mu}(\mathbf{k}_{//}) c_{l'\mu}^{n}(\mathbf{k}_{//}) \delta(E-\epsilon_n) \tag{8}$$

corresponding to a given value of $\mathbf{k}_{//}$.

Some typical examples of surface projected densities of states, $n_l(E)$ and $n_l(E, \mathbf{k}_{//})$ have been given in Ref.[18] for several vicinal surfaces of Rhodium. The most striking feature is the disappearance of almost all gaps. Indeed, as the width of the terraces increases, the area of the SBZ decreases and the height of the surface adapted Bulk Brillouin zone (BBZ), i.e., the sampled domain of bulk states (corresponding to all possible values of k_z) increases accordingly and corresponds to lines with no symmetry in the BBZ. This explains the absence of gaps and of true surface states. However a number of resonances can be identified. When the terrace width tends to infinity the spectral DOS becomes vanishingly small in the energy domain corresponding to gaps in the projected band structure of the flat surface with the same orientation as the terraces.

3.3. Surface and step energies

The calculation of the total energy of the slab, from which surface and step energies are deduced, involves a summation over the SBZ which is carried out by using special $\mathbf{k}_{//}$ points belonging to the irreducible part of the SBZ [33], each energy level being broadened by the derivative of a Fermi function of width w_f. The surface energy per surface atom of the vicinal surface is obtained from the following equation:

$$E_S(\mathbf{n}) = \frac{E_{slab}(\mathbf{n}) - N_{slab} E_{bulk}}{2} \tag{9}$$

where E_{slab} is the total energy of the slab (with N_{slab} layers) per surface unit cell and E_{bulk} is the energy of a bulk atom. The corresponding surface energy per unit area is thus $\gamma(\mathbf{n}) = E_S(\mathbf{n})/A(\mathbf{n})$ where $A(\mathbf{n})$ is the area of the surface unit cell.

The step energy per unit step length $\beta(\theta)$ of a vicinal surface is usually defined by the formula:

$$\gamma(\mathbf{n}) = \gamma(\mathbf{n_0}) cos(\theta) + \beta(\theta) sin(\theta)/h \tag{10}$$

where h is the inter-planar distance along the direction $\mathbf{n_0}$ normal to the terraces. Note that due to the presence of the array of steps with a period depending on θ, $\beta(\theta)$ is

expected to vary with θ as a result of step-step interactions. The value of the step energy for an isolated step is then obtained in the limit $\theta \to 0$. It is easy to show [34] that equation (10) can be transformed into a more convenient form:

$$E_{step}(\mathbf{n_0}, p) = E_S(\mathbf{n_0}, p) - (p - 1 + f)E_S(\mathbf{n_0}, \infty) \tag{11}$$

where $E_{step}(\mathbf{n_0}, p)$ is now the step energy per step atom of the vicinal surface in which the terraces of orientation $\mathbf{n_0}$ have p atomic rows parallel to the step edge (including the inner edge) and $E_S(\mathbf{n_0}, p)$ ($E_S(\mathbf{n_0}, \infty)$) is the surface energy per surface atom of the vicinal (flat) surface. Finally, f is a geometrical factor depending on the vicinal surface which has been defined in Sect.2 (Fig.1).

The calculation of step energies and especially of their variation with p is rather tricky since the step energies are of the order of a few 10^{-1} eV and the magnitude of their variation with p is, at most, $\simeq 2.10^{-2}$eV. Thus the surface energies involved in (11) must be calculated with an accuracy of 10^{-3}eV. The parametrized TB hamiltonian being given, the accuracy of the calculation is mainly governed by the thickness of the slab, the number of $\mathbf{k}_{//}$ points in the irreducible part of the SBZ and the Fermi level broadening w_f. Note that we have extrapolated the total energy at zero broadening using the usual approximation of Ref.[35]:

$$E_{tot}(T = 0) \approx E_{tot}(T) - \frac{1}{2}TS_e + O(T^2) \tag{12}$$

where S_e is the electronic entropy and T is the electronic temperature corresponding to the Fermi broadening w_f. We have found that the required accuracy is achieved when using a number of vicinal planes in the slab $N_{slab} = pn_{slab}$ with $n_{slab} \simeq 10$, 64 special $\mathbf{k}_{//}$ points and a Fermi level broadening of 0.2eV. Furthermore the iteration process ensuring the self-consistent charge neutrality condition has been stopped when the difference of charge between two consecutive iterations is $< 0.01e^-$ per atom and the difference in total energy smaller than 10^{-4}eV.

In Table 2 the surface energies per unit surface area $\gamma(\mathbf{n})$ and $E_S(\mathbf{n_0}, p)$ per surface atom are given as a function of p for the $p(100) \times (111)$ and $p(111) \times (100)$ surfaces. The step energies per step atom are deduced from (11) and are shown in Fig.2 as a function of p. Typically terraces with $p \geq 6$ are wide enough to get the asymptotic value, i.e., the isolated step energy with a numerical accuracy of $\simeq 10^{-3}$eV. The values of the isolated step energies for Rh, Pd and Cu are given in Table 3 for the four families of vicinal surfaces listed in Table 1.

Let us compare our results with those deduced from the effective pair potential model proposed by Vitos et al.[34]. In this model the energy of a bulk atom is written:

$$E_{bulk} = -\sum_{R_J < R_c} Z_b^J V_J \tag{13}$$

where Z_b^J is the number of J^{th} neighbors at the distance R_J for a bulk atom and R_c the cut-off radius of interactions, and the surface energy (per surface atom) is:

$$E(\mathbf{n_0}, p) = \sum_{R_J < R_c} n_S^J V_J, \tag{14}$$

	Rh (a=3.81Å)			
	$p(100)\times(111)$		$p(111)\times(100)$	
p	γ	E_S	γ	E_S
2	3.281	2.465	3.281	2.465
3	3.259	3.836	3.200	3.551
4	3.225	5.217	3.120	4.634
5	3.197	6.597	3.066	5.726
6	3.175	7.976	3.026	6.819
7	3.158	9.355	2.995	7.911
∞	3.044	1.379	2.781	1.091
	Pd (a=3.89Å)			
	$p(100)\times(111)$		$p(111)\times(100)$	
p	γ	E_S	γ	E_S
2	1.957	1.533	1.957	1.533
3	1.922	2.358	1.897	2.194
4	1.890	3.188	1.847	2.860
5	1.867	4.016	1.811	3.526
6	1.850	4.845	1.784	4.191
7	1.837	5.673	1.764	4.857
∞	1.754	0.828	1.625	0.665
	Cu (a=3.52Å)			
	$p(100)\times(111)$		$p(111)\times(100)$	
p	γ	E_S	γ	E_S
2	2.049	1.314	2.049	1.314
3	2.051	2.060	2.000	1.895
4	2.034	2.809	1.953	2.476
5	2.019	3.557	1.917	3.057
6	2.008	4.306	1.892	3.639
7	1.999	5.054	1.872	4.220
∞	1.935	0.748	1.734	0.581

Table 2. The surface energies $\gamma(J/m^2)$ and $E_S(eV/atom)$ of two families of vicinal surfaces. The surface area of the unit cell of a $p(100)\times(111)$ surface is $S=\sqrt{(2p-1)^2+2}\,a^2/4$ (a: lattice parameter) and the angle θ is given by $\tan\theta=\sqrt{2}/(2p-1)$. The corresponding quantities for the $p(111)\times(100)$ surface are: $S=\sqrt{(p+1)^2+2(p-1)^2}\,a^2/4$ and $\tan\theta=2\sqrt{2}/(3p-1)$.

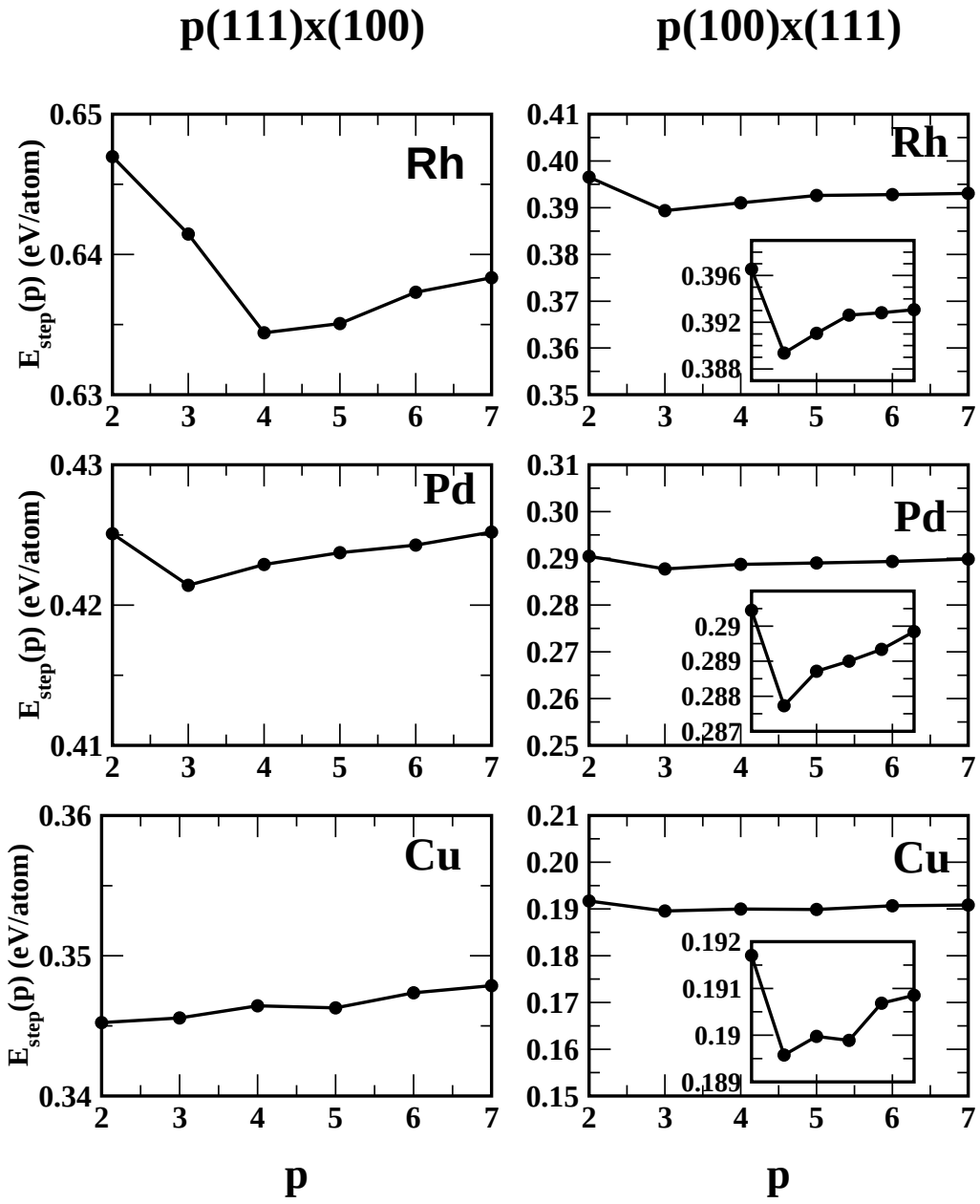

Figure 2. The variation of the step energy (per step atom) as a function of the terrace width for the $p(100) \times (111)$ (for which the energy scale has been enlarged in the insets to put forward clearly the sign of interactions) and $p(111) \times (100)$ vicinal surfaces of Rh, Pd and Cu.

	Vicinal surface	Step energy E_{step} (eV/atom)					
	$p \to \infty$	TB	EPP				
				TB	Vitos	Methfessel	Eichler	Galanakis
Rh	$p(111) \times (100)$	0.638	$2V_1 + 4V_3$	0.657	0.583	0.520	0.650	0.670
	$p(111) \times (\bar{1}11)$	0.645	$2V_1 + 4V_3$	0.657	0.583	0.520	0.650	0.670
	$p(100) \times (111)$	0.393	$V_1 + 2V_2$	0.407	0.288	0.265	0.295	0.285
	$p(100) \times (010)$	0.747	$2V_1 + 2V_2$	0.738	0.550	0.480	0.580	0.596
Pd	$p(111) \times (100)$	0.425	$2V_1 + 4V_3$	0.429	0.460	0.423		0.500
	$p(111) \times (\bar{1}11)$	0.432	$2V_1 + 4V_3$	0.429	0.460	0.423		0.500
	$p(100) \times (111)$	0.289	$V_1 + 2V_2$	0.295	0.106	0.222		0.298
	$p(100) \times (010)$	0.536	$2V_1 + 2V_2$	0.533	0.265	0.427		0.548
Cu	$p(111) \times (100)$	0.348	$2V_1 + 4V_3$	0.347	0.380			0.426
	$p(111) \times (\bar{1}11)$	0.345	$2V_1 + 4V_3$	0.347	0.380			0.426
	$p(100) \times (111)$	0.191	$V_1 + 2V_2$	0.192	0.200			0.241
	$p(100) \times (010)$	0.352	$2V_1 + 2V_2$	0.359	0.363			0.456

Table 3. Step energies for various vicinal geometries. Several types of results are presented: the full tight-binding (TB) calculation and calculations based on effective pair potentials V_1, V_2, V_3 (EPP) fitted on the (111), (100), and (110) surface energies obtained from various methods: tight-binding, and *ab-initio* methods (Vitos *et al.* [34], Methfessel *et al.* [36] and Eichler *et al.* [37]) and Galanakis *et al.* [38]

(terrace)×(ledge)	**Rh**	**Pd**	**Cu**		
			This work	**Other calculations**	**Experiments**
$(111) \times (100)$	0.339	0.249	0.143	0.092 [15]	0.113 ± 0.007 [1]
$(111) \times (\bar{1}11)$	0.329	0.242	0.148	0.117 [15]	0.121±0.007 [1]
$(100) \times (111)$	0.349	0.247	0.146	0.139 [54]	0.123[4] 0.129±0.009 [1]
V_1	0.332	0.238	0.166		

Table 4. Kink energies for various steps with closed-packed edges in Rh, Pd and Cu (in eV)

n_S^J is the total number of J^{th} neighbors (per surface atom) suppressed by the surface. The step energies are then given by:

$$E_{step}(\mathbf{n_0}, p) = \sum_{R_J < R_c} n_{step}^J(\mathbf{n_0}, p) V_J \tag{15}$$

with:

$$n_{step}^J(\mathbf{n_0}, p) = n_S^J(\mathbf{n_0}, p) - (p - 1 - f) n_S^J(\mathbf{n_0}, \infty) \tag{16}$$

where $n_S^J(\mathbf{n_0}, p)$ and $n_S^J(\mathbf{n_0}, \infty)$ are, respectively, the total number of neighbors (per surface atom) in the J^{th} coordination shell suppressed by the vicinal and flat surfaces. In Vitos et al. work [34] the effective pair potentials are limited to first, second and

third neighbors (V_1, V_2, V_3) and their numerical values are derived from the (111), (100) and (110) surface energies. These surface energies are calculated using ab-initio codes, the surface relaxation being neglected. Note that, due to the short range of the pair potentials, the numbers $n^J_{step}(\mathbf{n_0}, p)$ $(J \leq 3)$ are constant as soon as p exceeds a given value p_∞ which is actually very small, i.e., most often $p_\infty = 2$. As a consequence this model ignores step-step interactions. Our calculations allow to check the validity of this approach by using the pair potentials drawn from the surface energies obtained with the same parametrised TB hamiltonian. The expression for the step energies are given in Table 3 and their numerical values are very close to the values obtained from the previous method. Thus the method proposed by Vitos et al. is quite valid to derive a good estimate of the step energies when the low index surface energies and the step energy calculated from (11) are computed in the same manner. Indeed, we have compared our results with those obtained with the approach of Vitos et al. by using other data sets for the surface energies [34, 36, 37, 38]. It is seen in Table 3 that the agreement is reasonable save for Pd $p(100) \times (111)$ using the surface energy data set of Vitos et al. Actually, with the latter data V_2 is negative, while it is positive in the other calculations.

Finally note that in the effective pair potential model the step energy of vicinal surfaces with (111) terraces is the same for both ledge orientations (100), i.e., type A step and $(\bar{1}11)$, i.e., type B step (see Table 3) while in the full TB calculation step A is slightly energetically favoured for Rh and Pd, the reverse being found for Cu. This has some consequences on the equilibrium shape of large adislands in homoepitaxy as will be shown below.

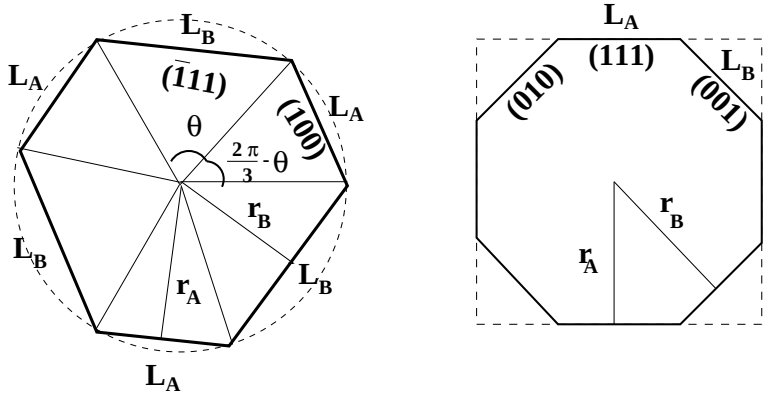

Figure 3. The equilibrium shapes of islands on (111) (a) and (100) (b) FCC surfaces. The orientations of the microfacets are indicated.

Let us now compare our results with experimental data. The ratio of step energies and their absolute values can be directly determined, by means of STM, from the observation, as a function of temperature, of the equilibrium shape of 2D adislands in homoepitaxy on a surface. On the (111) surface the adislands should show three-fold symmetry. Consequently their shape is hexagon-like with alternating A- and B-

type edge segments (see Fig.3). When the two step energies are equal, the A and B segments have equal lengths and the hexagon is regular. Otherwise the ratio L_A/L_B of the lengths of A and B segments can be derived from β_A/β_B by applying the Wulff theorem. Experimental results are only available for Cu. The most recent experiments by Giesen et al.[1] give an average step energy for the two kinds of steps on Cu(111) equal to 0.27 ± 0.03eV per step atom, the energy of step A being measurably $(1.1 \pm 0.7\%)$ larger than that of a B step. Other published results [39, 40] on the average step energy lie between 0.22 and 0.31eV. Our full TB calculations (see Table 3) is in very good agreement with experiments for the ratio β_A/β_B. However they seem to slightly overestimate the average step energy. On the (100) surface the adislands should show a four-fold symmetry. Accordingly, the most simple polygonal shapes are a perfect square with (111) type ledges or a square with broken corners with both (111) and (010) type ledges (resp. A and B, see Fig.3). It can be easily shown [18] that when $E^A_{step}/E^B_{step} \leq 1/2$ the equilibrium shape is a perfect square and a square with broken corners otherwise. The experimental results of Giesen et al.[1] show unambiguously square adislands with broken corners from which they deduce the ratio $E^A_{step}/E^B_{step} \simeq 0.57$ to be compared to our full TB calculations that gives 0.54. The calculated energy of the step $(100) \times (111)$ is 0.191eV, also in good agreement with the experimental results $(0.22 \pm 0.02$eV).

3.4. Step-step electronic interactions

Let us now discuss step-step interactions. There exists several types of interactions between steps. The most studied is the so-called elastic interaction due to the deformation fields around each step which interact repulsively. This elastic interaction gives rise in the continuum elasticity limit to an energy term varying at large inter-step distance as $1/d^2$ where d is the distance between two steps [41]. However, as we will see below (Sect.4.2), when trying to fit results derived from empirical potentials on relaxed surfaces, it appears that for smaller d ($d \leq 6$ inter-row spacings) the behavior of $E_{step}(d)$ deviates significantly from this law [42, 43, 44, 45]. Furthermore meandering steps cannot cross each other. This gives rise to an entropic repulsive interaction varying as $1/d^2$ at large d [46]. Charge transfers in the vicinity of the steps produce a dipole-dipole interaction (repulsive or attractive) varying also as $1/d^2$.

Finally oscillatory electronic interactions of the Friedel type (i.e., arising from the interference between electron density oscillations around steps which have been visualized by STM [47]) should also be present similarly to those existing between chemisorbed atoms or defects [48, 49] but they have attracted little attention, at least up to now. Such interactions have been invoked by Frohn *et al.* [50] to explain their STM observations on Cu(11n). They have been introduced theoretically for cubium with a TB s band by Redfield and Zangwill [51] and discussed in a phenomenogical manner by Pai *et al.* [2]. A calculation of these interactions for vicinal surfaces of W(110) has also been carried out using a modified fourth moment approximation to TB theory for a pure d band [52]. However, until recently there were no detailed electronic structure

calculations on this subject, except one preliminary attempt with a tight-binding scheme for FCC transition metals with a pure d band showing that these oscillatory interactions do exist [53]. General trends were put forward but the results were not quantitative due to the role played by sp electrons in the total energy, which is significant in FCC transition metals. The spd TB model described above avoids this approximation. Three main features can be extracted from Fig.2 (i) the step-step electronic interaction has a damped behavior which is most often oscillatory, (ii) the amplitude of the oscillations can be as large as some 10^{-2}eV for small values of p and remains of the order of some 10^{-3}eV when $p \geq 5$ in the studied domain of p, (iii) the shape of the oscillations is quite stable for two neighboring elements in the periodic table (Rhodium and Palladium) but it is dependent on the orientation of the steps.

Let us now compare our results with related works. The electronic step-step interaction energies are of the same order of magnitude as the full step-step interactions derived from experiments by using an analysis of terrace width distributions which most often assumes purely repulsive interactions varying as $1/d^2$. This suggests that, as already mentioned [2], this type of interactions should be included in the treatment of experimental data. Nevertheless, it remains difficult to fit our results by an analytical expression and extrapolate an asymptotic behavior to compare with elastic interactions.

Unfortunately they are only a few experimental data in the domain of small terrace widths. However, an anomalous behavior of the terrace width distribution at low temperatures for Cu $p(100) \times (111)$ has been observed by Frohn et al.[50] which could be interpreted as due to a repulsive interaction when $d \simeq 1-2$ (in units of the nearest neighbor distance) but attractive (or oscillatory) when $d \simeq 3-5$. This is quite consistent with our results (Fig.2).

Finally kink formation energies have been calculated within the same TB method [18] and the geometry suggested by Feibelman [15]. The results are given in Table 3 and compare favourably with existing experiments and other calculations [15, 54].

4. Vibrational properties of Cu vicinal surfaces

The presence of steps on a surface modifies the electronic structure (see Sect.3) as well as the vibrational states, compared to the flat surface with the same orientation as the terraces. In the following we will use an empirical potential to investigate the vibrational states of vicinal surfaces of copper and deduce the contribution of phonons to the free energy of steps.

4.1. The empirical potential.

The empirical potential used to describe the interatomic interactions of a set of atoms located at $\mathbf{R_i}$ is of the form:

$$V(\mathbf{R_1}, ...\mathbf{R_i}, ...) = A \sum_{i,j,j\neq i} (R_0/R_{ij})^p f_c(R_{ij})$$

$$- \xi \sum_i \Big[\sum_{j \neq i} \exp[-2q(R_{ij}/R_0 - 1)] f_c(R_{ij}) \Big]^{\alpha} \qquad (17)$$

where R_{ij} is the distance between atoms i and j, R_0 is a reference distance that we take equal to the bulk nearest neighbor spacing, $f_c(R) = 1/(1 + exp[(R - R_c)/\Delta])$ is a smooth cut-off function with a cut-off radius R_c and α is an exponent set equal to 2/3.

The parameters A, ξ, p and q are fitted to the experimental values of the cohesive energy E_c ($E_c = -3.5eV/at$) and of the three elastic constants, i.e., the bulk modulus ($B = 10.470eV/at$) and the two shear moduli C and C' ($C = 6.046eV/at, C' = 1.917eV/at$). The equilibrium equation at $R_0 = 2.5526$Å gives a relation between the four parameters.

We have determined by a least mean square fit the sets of parameters obtained with different radii R_c for which interactions are cut off beyond first, second, third and fourth neighbors. For each set of parameters we have compared the fitted values of E_c, B, C, C', the surface relaxation of low index surfaces and the bulk phonon spectra to experiments. Let us mention that we have also tried other sets of exponents for α but the choice of $\alpha = 2/3$ was greatly improving the surface energies compared to ab-initio data [23].

The best set of parameters is obtained for a cut-off radius $R_c = 4.02$Å between second and third neighbors and the corresponding parameters are: A=0.206eV, ξ=1.102eV, p=7.206, q=2.220. Indeed with this potential (hereafter referred to as P_2) the fit of E_c, B, C and C' is excellent (better than 1meV per atom). When the potential includes only first nearest neighbors the shear moduli are not well reproduced and, in particular, C is about 25% smaller than the experimental value. The inclusion of third and fourth neighbors has a smaller influence on the elastic constants but the general tendency is an underestimation of the inward surface relaxation as one increases the cut-off radius beyond the second neighbors. We must emphasize that surface relaxation is important to get the local modifications of force constants correctly.

To obtain the phonon dispersion curves in the harmonic approximation the dynamical matrix is calculated from the analytical expression of the potential (17) and diagonalized for wave vectors $\mathbf{k}$ following symmetry lines in the BBZ. The calculated bulk dispersion curves are presented in Fig 4. The agreement with experiment [55] is excellent. Apart from the top of the spectrum at points X and L where the deviation between calculated and experimental frequencies is around 0.2THz, everywhere else the deviation is less than 0.1THz. Note also that the shallow minimum at W in the lowest frequency band along XWX is reproduced only when R_c is chosen between second and third nearest neighbors.

We have also calculated the surface projected band structure of phonons for the three low index surfaces (111), (100) and (110) using the usual slab geometry. Our results were compared with available experimental EELS and IHAS data. The agreement is excellent for the three surfaces [23]. Low frequency as well as high frequency surface localized modes are reproduced with a surprising accuracy which is a good check of the transferability of the potential since surface modes are extremely sensitive to local

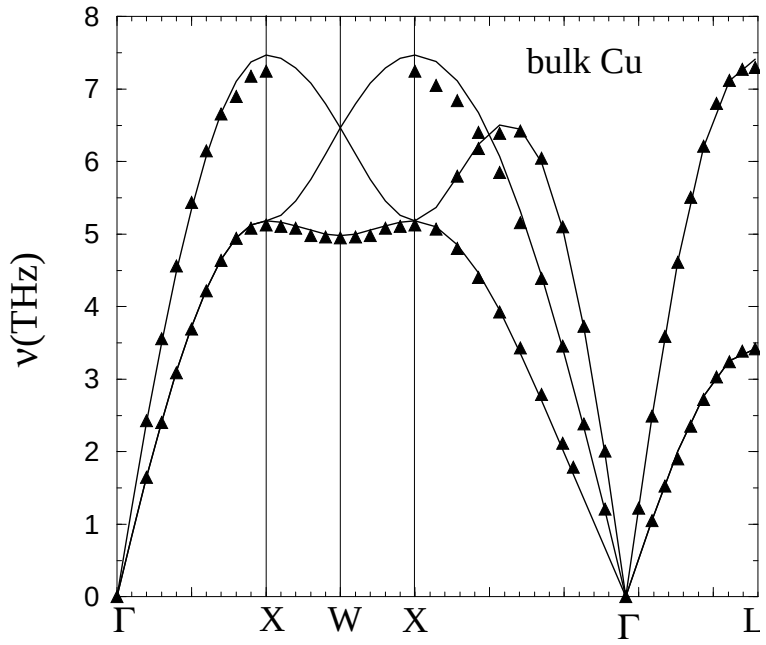

Figure 4. Phonon dispersion curves of bulk copper. The full lines correspond to the calculated dispersion curves and the triangles to the phonon frequencies measured from neutron inelastic-scattering experiments (Ref. [55]). Each segment along the path $\Gamma(\Delta)X(Z)W(Z)X(\Sigma)\Gamma(\Lambda)L$ is proportional to its length in reciprocal space.

modifications of the force constants due to the surface relaxation.

4.2. Atomic relaxation and elastic step-step interactions.

The first task is the determination of the equilibrium atomic structure which is obtained by a standard conjugate gradient method. A common feature for most metallic vicinal surfaces is that all atoms, save at the inner edge, relax inwards,i.e. , towards the bulk similarly to low index surfaces. However the direction of relaxation changes with the position p of the atomic row on the terrace and one can identify a vortex-like structure described in a recent paper by Prévot *et al.* [56] The outer edge step atom (SC: step chain) always shows the largest inward relaxation, therefore the distance between the outer edge atom and its first nearest neighbor having the bulk coordination (BNN) exhibits the largest contraction compared to the bulk equilibrium nearest neighbor distance. As will be seen later the shortening of SC-BNN bonds produces a stiffening of the associated force constant.The inner edge atoms, contrary to the other terrace atoms, relax outwards. Another common feature to all metallic vicinal surfaces is the profile of the multilayer relaxation, defined as the ratio of the distance between two adjacent atomic planes parallel to the vicinal surface with respect to the corresponding bulk inter-layer spacing. The multilayer relaxation always shows a damped oscillatory behavior with a period of oscillation equal to the vicinality p of the surface [23, 42].

The equilibrium structure of a vicinal surface with a given terrace width p being

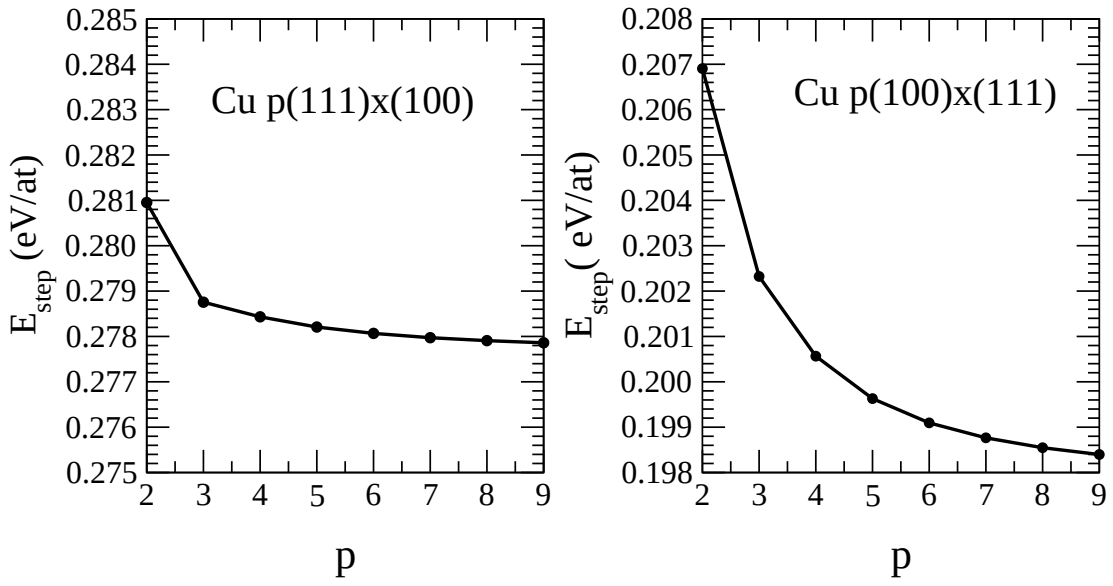

Figure 5. Variation of the step energy per step atom of the $p(100) \times (111)$ and $p(111) \times (100)$ vicinal surfaces as a function of the terrace width p. The geometry has been fully relaxed.

known, it is straightforward to calculate the corresponding step energy per atom $E_{step}(\mathbf{n_0}, p)$ using equation (11). $E_{step}(\mathbf{n_0}, p)$ is varying with the terrace width p as a result of step-step interactions. The step energy is obtained in the limit $p \to \infty$. In Fig. 5 we have presented the step energy per step atom for the vicinal $p(100) \times (111)$ and $p(111) \times (100)$ surfaces for p ranging from 2 to 9. $E_{step}(\mathbf{n_0}, p)$ is strictly decreasing when p increases as expected from a calculation based on a semi-empirical potential , since no oscillatory electronic effects are taken into account [18]. This variation is the result of purely elastic step-step interactions which are known to be repulsive from elasticity theory and, as mentioned previously, this term should vary at large inter-step distances as $1/d^2$ where d is the distance between two adjacent steps [41]. In order to compare the present results with the prediction of the elasticity theory we have fitted the step energy per step atom E_{step} as a function of $d = (p - 1 + f)a_0$ where a_0 is the distance between two adjacent atomic rows on the terrace plane $(6 \leq p \leq 100)$, with an expression of the form $A_0 + A_2/d^2 + A_3/d^3$. In the case of Cu $p(100) \times (111)$ surfaces, $f = 0.5$ and $a_0 = R_0$. The result is $A_0 = 0.198eV$, $A_2 = 0.322eV\text{Å}^2$ and $A_3 = -0.955eV\text{Å}^3$. A_0 is the asymptotic value giving the step energy of an isolated step and is in very good agreement with the value given by TB calculations (see Table 3). It is interesting to note that the coefficients A_2 and A_3 have opposite signs similarly to what was found on $p(100) \times (010)$ surfaces of Ni and Au in a previous atomistic study [57]. Although A_3 is

non-zero, its contribution becomes negligible for p larger than 10.

4.3. Projected phonon band structure of vicinal surfaces.

The vibrational spectra of various vicinal surfaces have been presented in a recent paper [23]. Thus, the most important features will be illustrated here on two specific cases for which detailed experimental IHAS [5] and EELS [6] data are available for phonons propagating parallel and perpendicular to the step edge on the (211) and (511) surfaces.

There are several common features on the surface projected band structure of vicinal surfaces. First the most striking feature is the disappearance of almost all gaps in any direction of $\mathbf{k}_{//}$ space, for the same reason as already explained in the electronic structure section. Second, the localized modes propagating perpendicular to the terraces have a clear back-folded structure. This back-folding leads to optical modes, their number increasing with the terrace width. Third, the localized modes propagating parallel to the step edge show strong similarity with the corresponding modes of the low index surface with the same terrace orientation. Finally some resonant or localized modes in the vicinity of the steps also appear. In particular, a very specific mode is present on almost all dispersion curves at the very top of the band edge. This state is purely localized on the BNN atoms and is closely related to the stiffening of the force constant mentioned above.

These general features are seen on the surface projected phonon band structure of the (211) and (511) surfaces, i.e., with Lang et al. notations $3(111) \times (100)$ and $3(100) \times (111)$. Indeed, in Fig.6, the only small noticeable gap is around the $\bar{X}$ point for the (211) surface, whereas all gaps have disappeared for the (511) surface. Let us consider the $\bar{\Gamma}\bar{X}$ and $\bar{\Gamma}\bar{Y}$ directions corresponding to directions of propagation parallel and perpendicular to the step edges, respectively. Along the $\bar{\Gamma}\bar{X}$ direction of the (211) surface, the most prominent surface features are a transverse mode (T) horizontally polarized, the sagittal Rayleigh mode (R) and a step localized mode (E). In addition another localized mode is found around the middle of the gap at $\bar{X}$. The same type of modes are also found on the (511) surface. Moreover there is a weakly localized longitudinal mode (L) which, actually, is also present on the (211) surface but is even less localized. All these results are in very good agreement with IHAS and EELS data. Modes propagating perpendicularly to the step (along $\bar{\Gamma}\bar{Y}$) can be qualitatively described as resulting from a "back-folding" [58] of the Rayleigh and transverse modes. Note that the mode localized on the BNN atom is particularly visible on the (511) surface for which the z component of the force constant between the BNN and step edge atom is 44% larger than the bulk one [23].

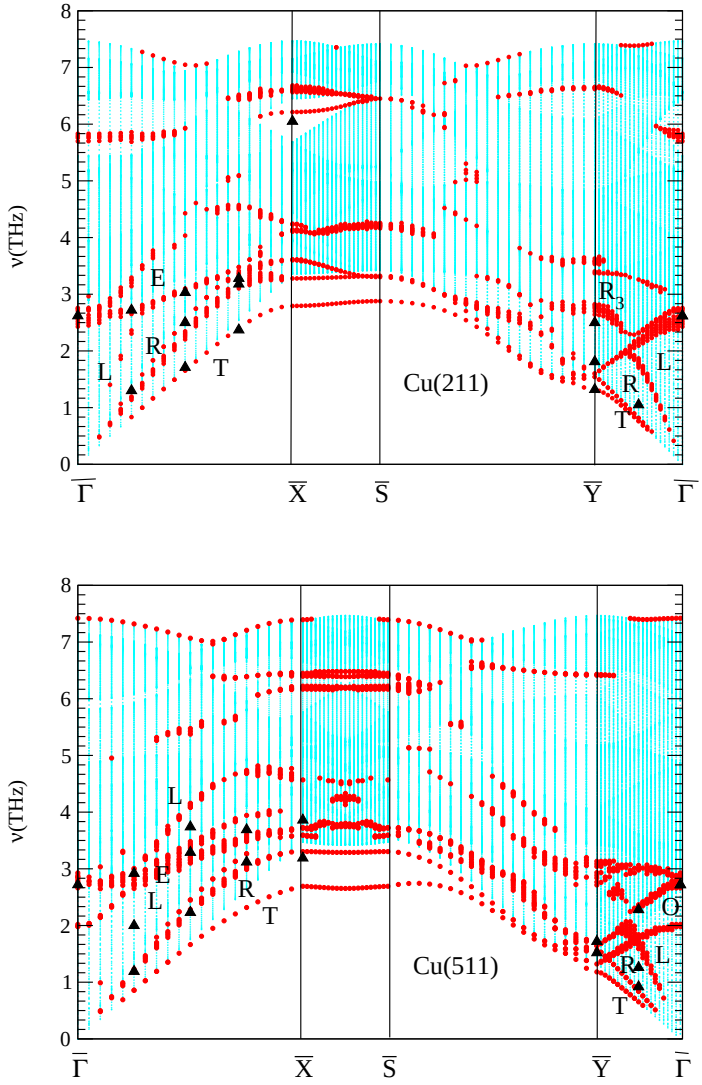

Figure 6. Frequency spectrum of phonons for the (211) (a) and (511) (b) surfaces of Cu as a function of $\mathbf{k}_{//}$ along a given path in the surface Brillouin zone. Each segment is proportional to its length in the reciprocal space. Bulk states are represented by small dots. Localized and resonant states are denoted by heavy dots. The prominent surface features are denoted with the same notations as in Ref.[5] and the localization criterion is 6% on the first four layers. Experimental points are taken from Ref.[5] except for the highest frequency at $\bar{X}$ which corresponds to the EELS data of Ref.[6].

4.4. Vibrational free energy of steps.

The contribution of vibrations to the free energy of a system which has a total density of frequencies $n(\nu)$ is given by:

$$F^{vib}(T) = k_B T \int_0^\infty \ln(2\sinh\frac{h\nu}{2k_BT})n(\nu)d\nu \qquad (18)$$

where k_B is the Boltzmann constant. In the case of 2D periodicity, the integral over the frequency is carried out by summing over special $\mathbf{k}_{//}$ points belonging to the irreducible SBZ. From the vibrational free energy of vicinal surfaces, low index surfaces and bulk, the vibrational free energy of steps (per step atom) $F^{vib}_{step}(T)$ can be derived at any temperature using an equation similar to (11). We have calculated $F^{vib}_{step}(T)$ for the $p(100) \times (111)$ and $p(111) \times (100)$ vicinal surfaces of increasing terrace widths, for temperatures ranging from 0 to 500K. The step vibrational free energy of a given vicinal surface is of the order of a few meV and decreases with temperature, reaching a linear regime for T larger than 100K when the entropy contribution becomes the leading term (see ref. [59]). More interestingly $F^{vib}_{step}(T)$ can be plotted for a given temperature, as a function of the terrace width as shown in Fig. 7.

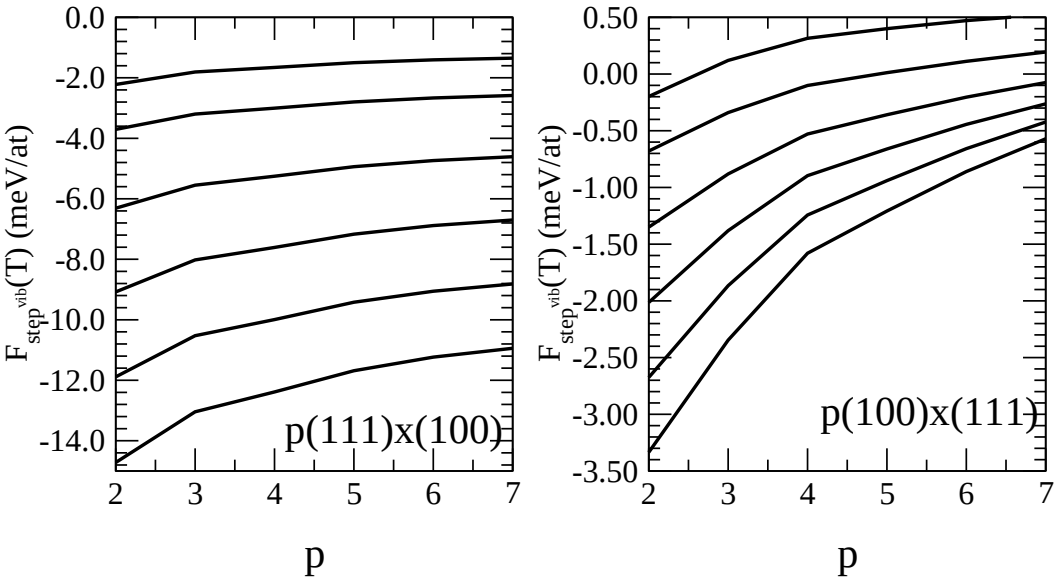

Figure 7. The contribution of vibrations to the step free energy for $p(100) \times (111)$ and $p(111) \times (100)$ vicinal surfaces as a function of p for given temperatures.

It appears that $F^{vib}_{step}(T)$ decreases in absolute value when the terrace width increases, i.e., phonons produce attractive step-step interactions. Furthermore the absolute value of these attractive step-step interactions increases with temperature. The possibility of interactions between surface defects mediated by phonons has already been investigated by Cunningham *et al.*[60] who have derived the phonon contribution to the free energy of interaction for an adatom pair on the (100) face of cubium using the Montroll-Potts model and also found an attractive interaction. Finally note that,

even though the vibrational contribution to the step energy is of the order of a few meV, therefore quite negligible compared to the absolute value of the step energy, its variation with the vicinality can be of the same order of magnitude as the repulsive elastic one at least in the range of small terrace widths ($p < 10$).

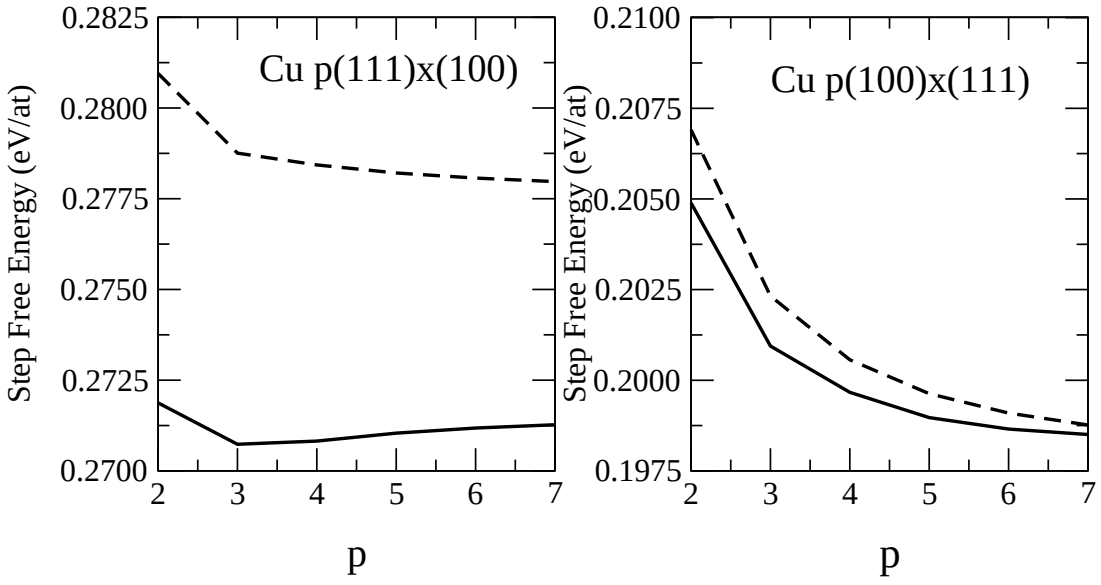

Figure 8. Variation of the step free energy at 300K as a function of p without (dashed line) and with (full line) the vibrational contribution.

Fig.8 shows the variation of the step energy as a function of p including both the elastic and vibrational contributions at 300K. The correction to the isolated step energy is small but phonons change the curvature of the step energy and, surprisingly, may even modify its sign. In particular for the $p(111) \times (100)$ surfaces the step energy exhibits a minimum at $p = 3$, i.e. , the resulting step-step interactions are attractive.

In addition, it must be kept in mind that electronic effects are far from being negligible, at least for small terrace widths (typically less than 10 atomic rows), and usually give rise to oscillatory interactions as shown in the previous sections.

5. Stability of vicinal surfaces with respect to faceting

Vicinal surfaces are not always stable. Indeed, as seen in Sect.3, their surface energies γ are large and it might be energetically favorable for the solid to expose to vacuum

low index facets with smaller surface energies per unit area, even if the total surface area is increased by the transformation. This phenomenon, called faceting, has been known for a long time [61]. The faceting condition implies the calculation of the surface energy for any surface orientation, i.e., the knowledge of the γ-plot. Herring [24] was the first to propose a geometrical construction starting from the γ-plot and predicting the occurrence of faceting. Then this condition was recast in a much simpler way (see Sect.5.1). The most simple methods for calculating the surface energies as a function of the orientation range from the crudest empirical pair potentials to various semi-empirical ones (EAM, EMT, SMA...), including an N-body contribution, which have been set up in the last two decades. Recently, the stability of vicinal surfaces with respect to faceting was reexamined using the EMT potential [62]. It was shown that the total energy difference between the vicinal and facetted surface is very small and, surprisingly, it was found that all vicinal surfaces between the (100) and (111) planes were unstable, at least at 0K, and that the observed stability at room temperature arises from the entropy contribution due to thermal vibrations. However, semi-empirical potentials have a common drawback: they only depend on the interatomic distances and not on the angular arrangement of atoms. Although this latter effect is small in metals, it is not obvious that it can be neglected in view of the tiny energy difference involved in faceting. In Refs.[25, 26], we have revisited this problem at 0K and analyzed the answers given by pair potentials, semi-empirical potentials and the TB calculations presented above (Sect.3). Finally our study of vibrational properties of vicinal surfaces (Sect.4) has enabled us to investigate the effect of finite temperatures.

In the following we first recall the faceting condition. Then we summarize our results concerning the possible faceting of the vicinal surfaces that are spanned when going from the (100) to the (111) plane. Other domains of orientations have been studied in [26].

5.1. Faceting condition of an infinite surface

Let us consider two low index surfaces Σ_1 and Σ_2 with normals $\mathbf{n_1}$ and $\mathbf{n_2}$, respectively, which intersect along a given row of atoms and the set of vicinal surfaces with equidistant step edges which is spanned when Σ_1 is rotated around the common atomic row towards Σ_2. Let us take Σ_1 as the origin of angles and denote θ_2 the angle ($\mathbf{n_1}$,$\mathbf{n_2}$). During this rotation the surfaces vicinal to Σ_1 are first found and the number of atomic rows p_1 (including the inner edge) on one terrace decreases from ∞ to 2 (angle θ_c). The surface corresponding to θ_c can also be regarded as a vicinal of Σ_2 with $p_2 = 2$. Then for $\theta_c \leq \theta < \theta_2$ the surfaces vicinal to Σ_2 are scanned with increasing terrace widths ($p_2 \geq 2$). An area S of any of these high index surfaces will transform into facets of normal $\mathbf{n_1}$ (area S_1) and normal $\mathbf{n_2}$ (area S_2) while keeping its average orientation when (Fig.9)

$$\gamma S > \gamma_1 S_1 + \gamma_2 S_2 \tag{19}$$

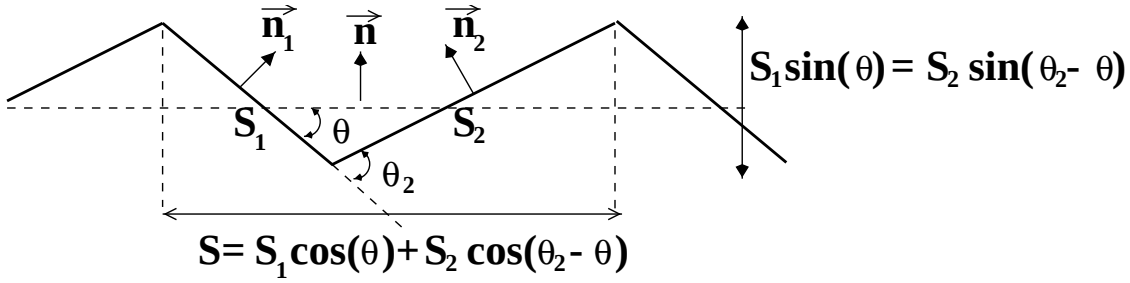

Figure 9. Faceting

(γ, γ_1 and γ_2 being the surface energies per unit area of the high index, Σ_1 and Σ_2 surfaces, respectively) with the constraints:

$$S = S_1 \cos\theta + S_2 \cos(\theta_2 - \theta) \tag{20}$$

$$S_1 \sin\theta = S_2 \sin(\theta_2 - \theta) \tag{21}$$

It is easily shown that the faceting condition can be written

$$f(\eta) > (1 - \eta/\eta_2) f(0) + (\eta/\eta_2) f(\eta_2) \tag{22}$$

with $\eta = \tan\theta$ and $f(\eta) = \gamma(\theta)/\cos\theta$. This condition is equivalent to the Herring construction [26].

This inequality has a simple geometrical interpretation: the vicinal surface corresponding to η is unstable(stable) when the point $(\eta, f(\eta))$ is above(below) the straight line D joining the points $(0, f(0))$ and $(\eta_2, f(\eta_2))$ or, equivalently, the sign of the deviation $\Delta f(\eta)$ from this straight line determines the stability ($\Delta f(\eta) < 0$) or the instability ($\Delta f(\eta) > 0$) of the vicinal surface. With straightforward geometrical considerations, it is easily shown [26] that:

$$\Delta f(\mathbf{n}) = [E_S(\mathbf{n}) - (p_1 - 1)E_S(\mathbf{n_1}) - (p_2 - 1)E_S(\mathbf{n_2})]/A_0(\mathbf{n}) \tag{23}$$

where $A_0(\mathbf{n})$ is the projected area of the surface unit cell A of the vicinal surface of orientation $\mathbf{n}$ on Σ_1. This formula applies as well in the domain $0 \leq \theta \leq \theta_c$ with $p_2 = 2$, as when $\theta_c \leq \theta \leq \theta_2$ with $p_1 = 2$. $E_S(\mathbf{n})$ is the surface energy (per atom) of the surface normal to $\mathbf{n}$. It is interesting to note that the condition of instability of the surface corresponding to η_c (normal $\mathbf{n_c}$) is simply:

$$E_S(\mathbf{n_c}) > E_S(\mathbf{n_1}) + E_S(\mathbf{n_2}) \tag{24}$$

we will see below that in many cases the sign of $\Delta f(\eta_c)$ determines the stability for the whole range $[0, \eta_2]$. It is clear that the sign of Δf is independent of the origin of angles, i.e., if Σ_1 is referred by the angle θ_1, since it is given by the sign of the expression between the square brackets in Eq.(23) which will be denoted as $\Delta E(p_1, p_2)$ in the following.

Let us denote A_1 (A_2) the area of the unit cell of Σ_1 (Σ_2). It is straightforward to show that:

$$\begin{cases} \Delta f(\eta) = \dfrac{\Delta E(p_1,2)}{A_2 \sin\theta_2}\eta & 0 \le \eta \le \eta_c \\ \Delta f(\eta) = \dfrac{\Delta E(2,p_2)}{A_1}(1-\eta/\eta_2) & \eta_c \le \eta \le \eta_2 \end{cases} \tag{25}$$

By using equation (11), $\Delta E(p_1, 2)$ can be transformed into:

$$\Delta E(p_1,2) = E_{step}(\mathbf{n}_1, p_1) - E_S(\mathbf{n}_2) + f_1 E_S(\mathbf{n}_1) \tag{26}$$

(a similar equation can be written for $\Delta E(2, p_2)$ by interchanging the indices 1 and 2 in the right hand side of this equation). As seen in Sect.3, the step energy varies with p due to step-step interactions and, consequently, $\Delta E(p_1, 2)$ and $\Delta E(2, p_2)$ depend on η. When these interactions are neglected, these last two quantities are equal to their values at $p_1 = 2$ and $p_2 = 2$, or $\eta = \eta_c$. Then from (25) $\Delta f(\eta)$ has a triangular shape (Fig.10).

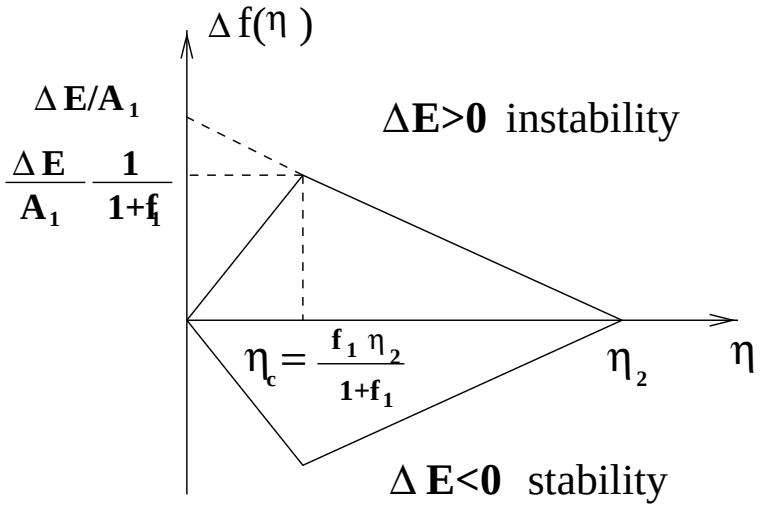

Figure 10. Behavior of $\Delta f(\eta)$ when there are no interactions between steps. η_c corresponds to $p_1 = p_2 = 2$.

Any vicinal between Σ_1 and Σ_2 is unstable(stable) relative to faceting when $\Delta E > 0 (\Delta E < 0)$. As a conclusion any deviation of $\Delta f(\eta)$ from the triangular shape is the sign of the presence of interactions between steps. If for a given orientation η_0 such that $0 < \eta_0 < \eta_c$, $\Delta f(\eta_0)$ is above(below) the tangent to $\Delta f(\eta)$ at the origin, then the interactions between steps are repulsive(attractive). The same conclusion holds for $\eta_c < \eta_0 < \eta_2$ but the tangent has to be taken at $\eta = \eta_2$. In the domain that will be considered below and defined by $\mathbf{n}_1(100)$ and $\mathbf{n}_2(111)$, i.e., $(100) - (111)$, η varies from 0 to $\eta_2 = \sqrt{2}$. When $0 < \eta \le \eta_c (\eta_c = \sqrt{2}/3)$ the crystallographic planes (2p-1,1,1) are spanned and correspond to the $p(100) \times (111)$ surfaces and when $\eta_c \le \eta < \eta_2$ ($\eta_2 = \sqrt{2}$) the crystallographic planes are (p+1,p-1,p-1) and the corresponding vicinal surfaces are

$p(111) \times (100)$ (see Table 1). Note that for $\eta = \eta_c$ the Miller indices of the surface are (311).

5.2. Stability of vicinal surfaces at 0K from semi-empirical potentials

Empirical potentials belonging to a very large class can be written as a sum of contributions E_i of each atom i (referred to the energy of a free atom, $E_i < 0$) depending on its environment of neighbors j at the interatomic distance R_{ij}, i.e.:

$$E = \sum_i E_i = \sum_i \Big\{ \sum_{j \neq i} V(R_{ij}) + F(\sum_{j \neq i} g(R_{ij})) \Big\} \tag{27}$$

E is the total energy of the system at 0K neglecting the zero point vibrational energy. In the following we set $\rho_i = \sum_{j \neq i} g(R_{ij})$. The first term of Eq.(27) is thus pairwise while the second one (in which g is a positive function) has an N-body character. The functions V and g are usually cut-off smoothly around a given radius R_c. This class of potentials includes pair potentials ($F(\rho_i) = 0$), potentials based on Effective Medium Theory (EMT)[8, 7], Embedded Atom Model (EAM)[9] and glue model [63], and potentials derived from the tight-binding approximation in the second moment approach ($F(\rho_i) \propto \sqrt{\rho_i}$) [10, 11, 12]or in which ($F(\rho_i) \propto \rho_i^{\alpha}$). This law with $\alpha = 2/3$ has been proposed to account for the effect of higher order moments [64] and has been actually found for Cu when fitting the five parameters of the potential to experimental bulk quantities (see Sect.4 and Ref.[23]). Note that in potentials of the tight-binding type, the N-body part is strictly attractive while the pairwise part is strictly repulsive.

Some physical insight can be gained by fixing the interatomic distances to their bulk equilibrium values, i.e., ignoring atomic relaxation effects. With this assumption $\sum_{j \neq i} V(R_{ij})$ and $\sum_{j \neq i} g(R_{ij})$ are linear combinations of the number of neighbors Z_i^J of atom i in the J^{th} coordination sphere of radius R_J ($R_J < R_c$) and $E_i = E(Z_i^1 ... Z_i^J ...)$. It is usual to take R_1 as the reference distance and set $g(R_1) = 1$. From the discussion of Sect.5.1, we will first determine if there is any interaction between steps. Obviously steps start to interact when the range of potential is large enough. Then the two straight lines of Fig.10 transform into as many segments (with discontinuities of slopes) as there are different step energies when p increases.

5.2.1. Pair potentials. These potentials are the simplest ones which have been used in the past. We will limit ourselves to the study of unrelaxed surfaces since it is well known that pair potentials most often lead to an outward relaxation instead of the inward one generally observed at metal surfaces. For any orientation of the surface it is easy to determine the coordination numbers $Z_i^1, Z_i^2, ...$for the successive atomic layers i from which the numbers n_{step}^J are deduced. For the domain $(100) - (111)$ it is found that there are no step interactions if $R_c < R_6$. Then $\Delta f(\eta)$ has the triangular shape of Fig.10 and its sign on the whole domain $[0, \eta_c]$ is given by (see Eq.(24))

$$\Delta E = E_S(311) - E_S(100) - E_S(111) = -4(V_3 + V_5) \tag{28}$$

As a conclusion if $R_c < R_3$, $\Delta E = 0$ so that the energy of any vicinal surface is equal to the energy of the faceted (100)/(111) surface. If $R_c < R_6$, the surface is unstable if $V_3 + V_5 < 0$ and stable otherwise.

5.2.2. N-body semi-empirical potentials. We now examine the case of semi-empirical potentials including an N-body contribution and begin by neglecting atomic relaxation in order to derive general trends for potentials of type (27). Then we will present a study of the stability of Cu vicinal surfaces in the $(100) - (111)$ domain using the semi-empirical potential set up in Sect.4.1.

When the interatomic distances are fixed to their bulk equilibrium values, the energy of an atom i, $E_i(Z_i^1, ...Z_i^J..)$, is no longer a linear function of Z_i^J. However, as will be seen below, the mathematical properties of the function has interesting physical consequences. It can be shown easily that the step energies of the $p(100) \times (111)$ and $p(111) \times (100)$ are independent of p as long as $R_c < R_3$ and are given by:

$$E_{step}^{p(100)\times(111)} = E(7,3) + E(10,5) - 3E(8,5)/2 - E(12,5)/2 \tag{29}$$

and:

$$\begin{aligned} E_{step}^{p(111)\times(100)} &= E(7,3) - 5E(9,3)/3 + E(10,5) + \\ &+ E(12,5) - 4E(12,6)/3 + \end{aligned} \tag{30}$$

Consequently for any semi-empirical potential of the form (27) including first and second nearest neighbors only, $\Delta f(\eta)$ has a triangular shape when atomic relaxation is neglected and its sign is given by:

$$\Delta E = E_S(311) - E_S(100) - E_S(111) \tag{31}$$

or:

$$\Delta E = [E(7,3) + E(10,5)] - [E(8,5) + E(9,3)] \tag{32}$$

Thus, in this approximation, ΔE arises from the difference of the sum of energies of, on the one hand, atoms belonging to the outer ($Z_i^1 = 7, Z_i^2 = 3$) and inner ($Z_i^1 = 10, Z_i^2 = 5$) step edges, and on the other hand, of $(100)(Z_i^1 = 8, Z_i^2 = 5)$ and $(111)(Z_i^1 = 9, Z_i^2 = 3)$ surface atoms.

As shown in Sect.5.2.1 the pair potential, when limited to second nearest neighbors, does not contribute to ΔE. Noting that, since we have chosen $g(R_1) = 1$, $\rho_i = Z_i^1 + Z_i^2 g_2$ with $g_2 = g(R_2)$, then we get:

$$\Delta E = [F(7 + 3g_2) - F(9 + 3g_2)] - [F(8 + 5g_2) - F(10 + 5g_2)] \tag{33}$$

For all the existing potentials of the form (27) $F''(\rho) = d^2F/d\rho^2$ is positive. As a consequence $F(\rho - 2) - F(\rho)$ is a decreasing function of ρ, therefore ΔE (and thus $\Delta f(\eta)$) is always positive in the whole domain. This common property of this class of

potentials has a clear physical origin: the energy E_i of an atom i should decrease more and more slowly when its coordination increases towards the bulk coordination [59, 65]. This clearly implies that $F''(\rho)$ must be positive. We have then proved that for *any* semi-empirical potential of the general form (27) on a rigid lattice at 0K and a cut-off radius $R_c < R_3$, *any* metal vicinal surface between (100) and (111) is *unstable* with respect to faceting.

So far we have demonstrated general results on the stability of vicinal surfaces neglecting atomic relaxation. These results were obtained under the assumption that the range of the potential is restricted to the first two shells of neighbors. As shown in Ref.[26] it is not possible to derive a general behavior when the range of interactions is extended to further neighbors. In order to investigate the effect of atomic relaxation and of the range of interactions, it is necessary to have an explicit expression of the potential. We will now present the results obtained for Cu with the semi-empirical potential (P_2) of Sect.4 whose range is limited to first and second neighbors. In addition we have also considered the potential (P_4) of the same type ($\alpha = 2/3$) but with a cut-off radius between fourth and fifth neighbors with parameters obtained from a least mean square fit of the cohesive energy, the three elastic constants and the bulk equilibrium distance. In all cases the atomic structure of each vicinal surface has been fully relaxed using a conjugate gradient algorithm.

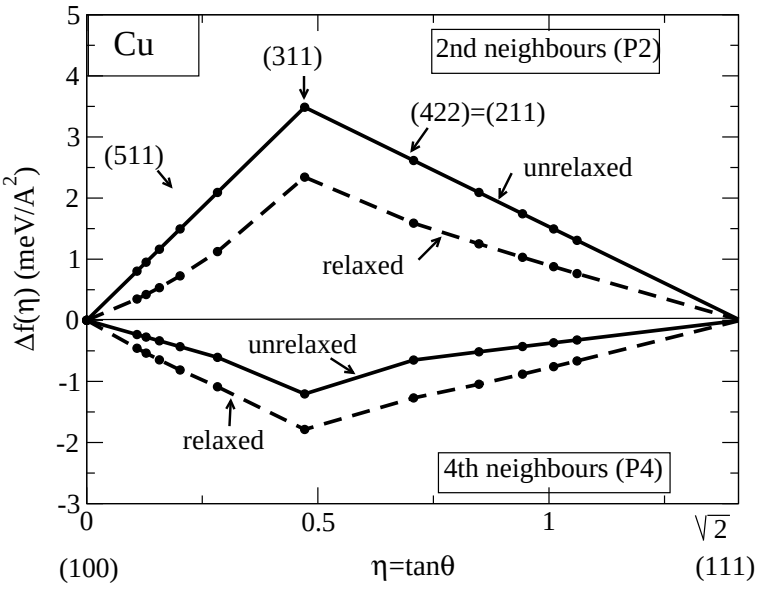

Figure 11. $\Delta f(\eta)$ for Cu derived from the semi-empirical potentials P_2 and P_4 given in the text corresponding to two cut-off radii with and without relaxation for the (100) - (111) domain.

The results are given in Fig.11 for the $(100) - (111)$ domain using both potentials and relaxed as well as unrelaxed surfaces. As predicted from our previous analysis in the unrelaxed case $\Delta f(\eta)$ has a triangular shape and is positive if the range of the potential is restricted to second neighbors (P_2). However, as expected, due to the effect

of farther neighbors $\Delta f(\eta)$ deviates from a triangular shape with potential P_4 and, more surprisingly, it changes sign. Thus all vicinal surfaces between (100) and (111) become stable.

Finally, atomic relaxation always acts in favor of the stabilization of vicinal surfaces since the atomic displacements are larger on a vicinal surface than on a flat one (see Sect.4). Nevertheless this effect is not large enough to modify the stability or instability of the vicinal surfaces. Furthermore, as clearly seen when using potential P_2 in the relaxed case, $\Delta f(\eta)$ has no longer a triangular shape and is entirely located above the triangle built from its tangent at both ends due to the repulsive elastic step-step interactions (see Sect.4).

Let us discuss and summarize our results. From our analytical study and Fig.11 it appears that the range of the potential plays an important role but it is difficult to draw general conclusions. In all cases considered here the effect of farther neighbors is to act in favor of the stabilization of vicinal surfaces, however including them will not automatically make vicinal surfaces stable, this crucially depends on their relative importance and, therefore, on the dependence of the functions $V(r)$ and $g(r)$ with distance in (27). The stability also depends on the relative importance of V with respect to $F(\rho)$ since, when farther neighbors are included, both terms are present in the energy balance. Moreover, in EAM and EMT potentials the N-body and pair parts are not necessarily purely attractive or purely repulsive, therefore even the sign of these terms is not known. Let us finally compare our results with those of Frenken and Stoltze [62]. These authors have calculated $\Delta f(\eta)$ for the fully relaxed (100) and (111) vicinal surfaces of Ag (and other metals) using an EMT potential with $R_3 < R_c < R_4$ but in which the contribution of third neighbors is nearly negligible. This explains the strong similarity between our results on relaxed Cu (Fig. 11) with potential P_2 and those of Frenken and Stoltze for Ag.

As a conclusion, the instability of vicinal surfaces at 0K claimed by these authors is an *unavoidable* consequence of the type of potential used when interactions are limited to first and second neighbors.

5.3. Stability of vicinal surfaces at 0K from tight-binding calculations.

It is interesting to deduce the function $\Delta f(\eta)$ from the results presented in Sect.3. Indeed, the TB calculations are certainly more realistic than those based on semi-empirical potentials since they account for the influence of the angular arrangement of neighbors and include electronic step-step interactions (often oscillatory). We have seen in Sect.3 that these interactions are small. However they may play a role in the very delicate energy balance which governs the stability of vicinal surfaces.

The functions $\Delta f(\eta)$ for Rh, Pd and Cu in the $(100) - (111)$ domain are plotted in Fig.12 and show very different behaviors depending on the chemical element. For Cu all vicinal surfaces in the domain are stable at 0K while for Pd they are unstable. Rh behaves quite differently: even though all vicinal surfaces are stable with respect

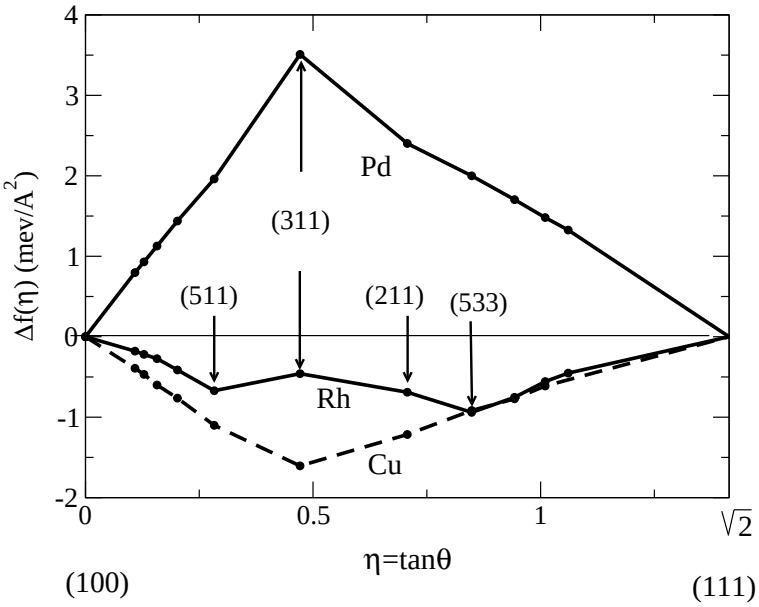

Figure 12. $\Delta f(\eta)$ for Rh, Pd and Cu from tight-binding calculations for the (100) - (111) domain.

to faceting into (100) and (111) facets, the vicinal surfaces of orientation such that $\sqrt{(}2)/5 < \eta < 3\sqrt{(}2)/5$ are unstable relative to faceting into (511) and (533) orientations which correspond to the two local minima in $\Delta f(\eta)$. This peculiar behavior is clearly related to the electronic step-step interactions which are repulsive for the (311) and (211) surfaces and attractive for (511) and (533) surfaces (see Fig.2).

5.4. Finite temperature effects.

So far all calculations were carried out at 0K. Therefore it is important to know whether the effect of a finite temperature may be large enough to reverse the stability of vicinal surfaces with respect to faceting. The variation of $f(\eta)$ with temperature arises from two contributions: the vibrational effects that have been studied in Sect.4 and the meandering of steps, which is regulated by the kink formation energy, giving rise to entropy contributions. Let us first discuss the order of magnitude of the latter. In the limit of infinite terraces steps fluctuate independently of each other but when the terrace width decreases the entropy gain due to the meandering is limited by the non-crossing condition which gives rise to a repulsive step-step interaction. Actually, both effects are driven by a parameter $\zeta = exp(-\epsilon_{kink}/k_BT)$ where ϵ_{kink} is the kink formation energy. As can be seen from Table 4 this parameter is quite small, at least up to room temperature, and, as a consequence,these two contributions are negligible compared with the value of $\Delta f(\eta)$ at 0K and they are also small compared with the contribution $\Delta f_{vib}(\eta)$ due to vibrations [26].

From the study of vibrations presented in Sect.4, we can easily derive $\Delta f_{vib}(\eta)$ as a function of temperature in the $(100) - (111)$ domain. The corresponding curves

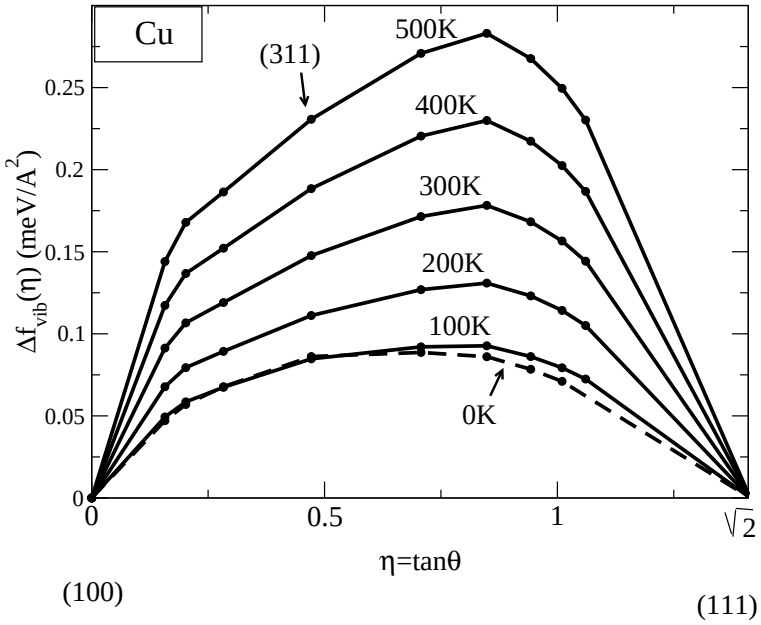

Figure 13. $\Delta f_{vib}(\eta)$ in the (100) - (111) domain from potential P_2 as a function of temperature.

for copper is drawn in Fig.13. It can be seen that Δf_{vib} is positive but its order of magnitude is not large enough to destabilize the vicinal surfaces of Cu in this domain. These results are in contradiction with those of Frenken and Stoltze [62]. Actually these authors evaluated the vibrational entropy contribution using a simplified Einstein model and neglected the vibrational internal energy which is justified at room temperature, but not at low temperature. Moreover they only included the perturbation between the outer edge and a (111) surface atom and not the term coming from the perturbation between the inner edge and the (100) surface atom (see Eq.(32)). These two terms are of opposite sign and are expected to be of the same order of magnitude. Consequently not only the estimate of Δf_{vib} in [62] is too large but even the sign is wrong.

In conclusion, the contribution of vibrations Δf_{vib} to Δf is quite small. Thus its calculation needs a precise knowledge of the phonon spectra including both vibrational internal energy and entropy, at least if the temperature varies from 0K to $\simeq$ 300K.

6. Conclusion

In conclusion, with the *spd* tight-binding method it is possible to carry out realistic calculations on the energetics of vicinal surfaces: surface, step and kink energies. Indeed, the formation energies of isolated steps, obtained with this method, on Rh, Pd and Cu surfaces for various geometries are in good agreement with existing experimental data. In particular, our results predict that an adisland of Cu on Cu(100) should be a square with broken corners at 0K. Moreover the correct relative stability of the two types of steps (A and B) on the vicinal surfaces of Cu(111) is obtained. Kink energies have also

been calculated and compare nicely with experimental data.

Following the approach of Vitos et al [34] and from the knowledge of the surface energies of the three low index surfaces calculated from the *spd* TB hamiltonian, effective pair interactions can be deduced giving step and kink energies in good agreement with those derived from the diagonalization of the same hamiltonian for vicinal surfaces. However in this approach step-step interactions are disregarded. On the contrary, our study, based on the calculation of step energies on vicinal surfaces as a function of the terrace width, has enabled us to derive electronic step-step interactions for narrow and moderately wide terraces ($d \leq 20$Å). These interactions are rapidly decaying and they may be attractive or repulsive depending on the terrace width. Moreover, in this range of widths, their order of magnitude is comparable to that of other interactions.

A semi-empirical potential for Copper, including an N-body contribution, has been built. It accounts for the multilayer relaxation of vicinal surfaces and describes accurately their localized vibration modes observed in IHAS and EELS. The contribution of vibrations to the free energy of steps has also been calculated as a function of the distance between steps and it was found that the step-step interactions mediated by phonons are attractive for Cu vicinal surfaces in the (100)-(111) domain.

The stability of vicinal surfaces with respect to faceting has also been investigated. The conclusions derived from semi-empirical potentials have been criticized. Contrary to the results obtained from these potentials which predict that vicinal surfaces of metals are unstable at 0K, the tight-binding electronic structure calculations lead to a variety of behaviors: a vicinal surface in the (100)-(111) domain may be stable (Cu) or unstable (Pd) relative to faceting into (100) and (111) facets or may even undergo a faceting towards other vicinal surfaces (Rh). Finally, temperature effects have been found to be negligible for Cu, at least up to room temperature.

[1] Giesen M 2001 *Prog. Surf. Sci.* **68** 1 and references therein
[2] Pai W W, Ozcomert J S, Bartelt N C, Einstein T L and Reutt-Robey J E 1994 *Surf. Sci.* **307-309** 747.
[3] Villain J, Grempel D R and Lapujoulade J 1985 *J. Phys.* F **15** 809
[4] Barbier L, Masson L, Cousty J and Salanon B 1996 *Surf. Sci.* **345** 197
[5] Witte G, Braun J, Lock A and Toennies J P 1995 *Phys. Rev.* B **52** 2165
[6] Kara A, Staikov P, Rahman T S, Radnik J, Biagi R and Ernst H J 2000 *Phys. Rev.* B **61** 5714
[7] Jacobsen K W, Norskov J K and Puska M J 1987 *Phys. Rev.* B**35** 7423
Jacobsen K W, Stoltze P and Norskov J K 1996 *Surf.Sci.* **366** 394
[8] Stoltze P 1994 *J. Phys.: Condens. Matter* **6** 9445
[9] Daw M S and Baskes M I 1984 *Phys. Rev.* B **29** 6443
[10] Ducastelle F 1970 *J. Physique* **31** 1055
[11] Sutton A P and Chen J 1984 *Philos. Mag. Lett.* **61** 139
[12] Finnis M W and Sinclair J E 1984 *Philos. Mag.* A**50** 45
[13] Nelson J S and Feibelman P J 1992 *Phys. Rev. Lett.* **68** 2188
[14] Stumpf R and Scheffler M 1996 *Phys. Rev.* B **53**, 958
[15] Feibelman P J 1999 *Phys. Rev.* B **60** 11118.
[16] Spisák D 2001 *Surf. Sci.* **489** 151
[17] Feibelman P J 2000 *Surf. Sci.* **463** L661
[18] Raouafi F, Barreteau C, Desjonquères M C and Spanjaard D 2002 *Surf. Sci.* **505** 183.
[19] Chen Y, Tong S Y, Kim J S, Kesmodel L S, Rodach T, Bohnen K P and Ho K M 1991 *Phys. Rev.* B **44** 11394
[20] Wei C Y, Lewis S P, Mele E J and Rappe A M 1998 *Phys. Rev.* B **57** 10062
[21] Kara A, Durukanoglu S and Rahman T S 1996 *Phys. Rev.* B **53** 15489
[22] Sklyadneva I Yu, Rusina G G and Chulkov E V 1998 *Surf. Sci.* **416** 17
[23] Barreteau C, Raouafi F, Desjonquères M C and Spanjaard D 2002 *Surf. Sci.* **519** 15.
[24] Herring C 1951 *Phys. Rev.* **82** 87
[25] Desjonquères M C, Spanjaard D, Barreteau C and Raouafi F 2002 *Phys. Rev. Lett.* **88** 056104
[26] Raouafi F, Barreteau C, Spanjaard D and Desjonquères M C 2002 *Phys. Rev.* B **66** 045410
[27] Lang B, Joyner R W and Somorjai G A 1972 *Surf. Sci.* **30** 440
[28] Mehl M J and Papaconstantopoulos D A 1996 *Phys. Rev.* B **54** 4519
[29] Barreteau C, Spanjaard D and Desjonquères M C 1998 *Phys. Rev.* B **58** 9721
[30] Slater J C and Koster G F 1954 *Phys. Rev.* **94** 1498
[31] Barreteau C, Guirado-López R, Spanjaard D, Desjonquères M C and Oleś A M 2000 *Phys. Rev.* B **61** 7781
[32] The parameters of reference [28] are available on the web-site http://cst-www.nrl.navy.mil/bind/
[33] Cunningham S L 1974 *Phys. Rev.* B **10** 4988
[34] Vitos L, Skriver H L and Kollar J 1999 *Surf. Sci.* **425** 212
[35] Weinert M and Davenport J W 1992 *Phys. Rev.* B **45** 13709
[36] Methfessel M, Henning D and M. Scheffler M 1992 *Phys. Rev.* B **46** 4816
[37] Eichler A, Hafner J, Furthmüller J and Kresse G 1996 *Surf. Sci.* **346** 300
[38] Galanakis I, Bihlmayer G, Bellini V, Papanikolaou N, Zeller R, Blügel S and Dederichs P H 2002 *Europhys. Lett.* **58** 751;
Galanakis I, Papanikolaou N and Dederichs P H 2002 *Surf. Sci.* **511** 1
[39] Schlösser D C, Verheij L K, Rosenfeld G and Comsa G 1999 *Phys. Rev. Lett.* **82** 3843
[40] Icking-Konert G S, Giesen M and Ibach H 1999 *Phys. Rev. Lett.* **83** 3880
[41] Marchenko V I and Parshin Y A 1981 *Sov. Phys. JETP* **52** 129
[42] Tian Z T and Rahman T S 1993 *Phys. Rev.* B **47** 9751
[43] Wolf D and Jaszczaki J 1992 *Surf. Sci.* **277** 301
[44] Najafabadi R and Srolovitz D J 1994 *Surf. Sci.* **317** 221
[45] Hecquet P and Salanon B 1996 *Surf. Sci.* **366** 415

[46] Jayaprakash C, Rottman C and Saam W F 1984 *Phys. Rev.* B **30** 6549
[47] Hasegawa Y and Avouris P H 1993 *Phys. Rev. Lett.* **71** 1071
[48] Einstein T L and Schrieffer J R 1973 *Phys. Rev.* B **7** 3629
[49] Yaniv A 1981 *Phys. Rev.* B **24** 7093
[50] Frohn J, Giesen M, Poensgen M, Wolf J F and Ibach H 1991 *Phys. Rev. Lett.* **67** 3543
[51] Redfield A C and Zangwill A 1992 *Phys. Rev.* B **46** 4289
[52] Wei Xu, Adams J B and Einstein T L 1996 *Phys. Rev.* B **54** 2910
[53] Papadia S, Desjonquères M C and Spanjaard D 1996 *Phys. Rev.* B **53** 4083
[54] Liu C L and Adams J B 1993 *Surf. Sci.* **294** 211
[55] Nicklow R M, Gilat G, Smith H G, Raubenheimer L J and Wilkinson M K 1967 *Phys. Rev.* **64** 922
[56] Prévot G, Cohen C, Schmaus D, Hecquet P and Salanon B 2002 *Surf. Sci.* **506** 272
[57] Shilkrot L E and Srolovitz D J 1996 *Phys. Rev.* B **53** 11120
[58] Armand G and Masri P 1983 *Surf. Sci.* **130** 89
[59] Desjonquères M C and Spanjaard D 1996 *Concepts in Surface Physics* (Heidelberg: Springer-Verlag)
[60] Cunningham S L, Dobrzynski L and Maradudin A A 1973 *Phys. Rev.* B **7** 4643
[61] Rosenhain W 1902 *Proc. Roy. Soc.* A **70** 252
[62] Frenken J W M and Stoltze P 1999 *Phys. Rev. Lett.* **82**, 3500
[63] Ercolessi F, Parrinello M and Tosatti E 1988 *Philos. Mag.* A **58** 213
[64] Guevara J, LLois A M and Weismann M 1995 *Phys. Rev,* B **52** 11509
[65] Robertson I J, Payne M C and Heine V 1991 *Europhys. Lett.* **15** 301